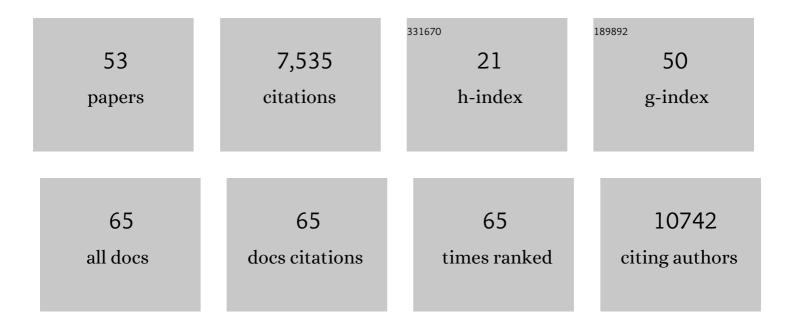
Yao Zhao

List of Publications by Year in descending order

Source: https://exaly.com/author-pdf/3799710/publications.pdf Version: 2024-02-01



#	Article	IF	CITATIONS
1	Crystal structure of SARS-CoV-2 main protease in complex with protease inhibitor PF-07321332. Protein and Cell, 2022, 13, 689-693.	11.0	136
2	ToF-SIMS characterization of surface chemical evolution on electrode surfaces educed by electrochemical activation. Journal of Analytical Atomic Spectrometry, 2022, 37, 890-897.	3.0	1
3	G-quadruplex inducer/stabilizer pyridostatin targets <i>SUB1</i> to promote cytotoxicity of a transplatinum complex. Nucleic Acids Research, 2022, 50, 3070-3082.	14.5	6
4	Hydrogen Isotope Effects on Aqueous Electrolyte for Electrochemical Lithiumâ€ion Storage. Angewandte Chemie - International Edition, 2022, 61, .	13.8	13
5	Structural basis for replicase polyprotein cleavage and substrate specificity of main protease from SARS-CoV-2. Proceedings of the National Academy of Sciences of the United States of America, 2022, 119, e2117142119.	7.1	64
6	Serum phosphopeptide profiling for colorectal cancer diagnosis using liquid chromatography–mass spectrometry. Rapid Communications in Mass Spectrometry, 2022, 36, e9316.	1.5	0
7	Open-flow microperfusion combined with mass spectrometry for <i>in vivo</i> liver lipidomic analysis. Analyst, The, 2021, 146, 1915-1923.	3.5	1
8	Photo-induced mitochondrial DNA damage and NADH depletion by –NO ₂ modified Ru(<scp>ii</scp>) complexes. Chemical Communications, 2021, 57, 4162-4165.	4.1	11
9	A Near-Infrared-II Polymer with Tandem Fluorophores Demonstrates Superior Biodegradability for Simultaneous Drug Tracking and Treatment Efficacy Feedback. ACS Nano, 2021, 15, 5428-5438.	14.6	79
10	High-throughput screening identifies established drugs as SARS-CoV-2 PLpro inhibitors. Protein and Cell, 2021, 12, 877-888.	11.0	95
11	Inhibition mechanism of SARS-CoV-2 main protease by ebselen and its derivatives. Nature Communications, 2021, 12, 3061.	12.8	149
12	Real-Time Characterization of the Fine Structure and Dynamics of an Electrical Double Layer at Electrode–Electrolyte Interfaces. Journal of Physical Chemistry Letters, 2021, 12, 5279-5285.	4.6	12
13	Identification of proteasome and caspase inhibitors targeting SARS-CoV-2 Mpro. Signal Transduction and Targeted Therapy, 2021, 6, 214.	17.1	17
14	Elevated CO2 concentration affects survival, but not development, reproduction, or predation of the predator Hylyphantes graminicola (Araneae: Linyphiidae). Environmental Pollution, 2021, 288, 117791.	7.5	0
15	Modest sexual size dimorphism and allometric growth: a study based on growth and gonad development in the wolf spider <i>Pardosa pseudoannulata</i> (Araneae: Lycosidae). Biology Open, 2021, 10, .	1.2	1
16	Transcriptome responses to elevated CO 2 level and Wolbachia â€infection stress in Hylyphantes graminicola (Araneae: Linyphiidae). Insect Science, 2020, 27, 908-920.	3.0	1
17	Cisplatinâ€induced alteration on membrane composition of A549 cells revealed by ToFâ€SIMS. Surface and Interface Analysis, 2020, 52, 256-263.	1.8	9
18	Atmospheric particulate characterization by ToF-SIMS in an urban site in Beijing. Atmospheric Environment, 2020, 220, 117090.	4.1	8

ΥΑΟ ΖΗΑΟ

#	Article	IF	CITATIONS
19	ToFâ€&IMS analysis of chemical composition of atmospheric aerosols in Beijing. Surface and Interface Analysis, 2020, 52, 272-282.	1.8	3
20	Structural insights into substrate recognition by the type VII secretion system. Protein and Cell, 2020, 11, 124-137.	11.0	25
21	Photoactivatable diazido Pt(iv) anticancer complex can bind to and oxidize all four nucleosides. Dalton Transactions, 2020, 49, 17157-17163.	3.3	7
22	Reactions of a photoactivatable diazido Pt(iv) anticancer complex with a single-stranded oligodeoxynucleotide. Dalton Transactions, 2020, 49, 11249-11259.	3.3	7
23	Tandem Mass Spectrometry Reveals Preferential Ruthenation of Thymines in Human Telomeric G-Quadruplex DNA by an Organometallic Ruthenium Anticancer Complex. Organometallics, 2020, 39, 3315-3322.	2.3	6
24	<i>In Situ</i> Visualization of Proteins in Single Cells by Time-of-Flight–Secondary Ion Mass Spectrometry Coupled with Genetically Encoded Chemical Tags. Analytical Chemistry, 2020, 92, 15517-15525.	6.5	11
25	Breaking the Intracellular Redox Balance with Diselenium Nanoparticles for Maximizing Chemotherapy Efficacy on Patient-Derived Xenograft Models. ACS Nano, 2020, 14, 16984-16996.	14.6	105
26	Cryo-EM snapshots of mycobacterial arabinosyltransferase complex EmbB2-AcpM2. Protein and Cell, 2020, 11, 505-517.	11.0	13
27	Structural basis for the inhibition of SARS-CoV-2 main protease by antineoplastic drug carmofur. Nature Structural and Molecular Biology, 2020, 27, 529-532.	8.2	339
28	Structure of Mpro from SARS-CoV-2 and discovery of its inhibitors. Nature, 2020, 582, 289-293.	27.8	3,133
29	Unexpected Thymine Oxidation and Collision-Induced Thymine-Pt-guanine Cross-Linking on 5′-TpG and 5′-GpT by a Photoactivatable Diazido Pt(IV) Anticancer Complex. Inorganic Chemistry, 2020, 59, 8468-8480.	4.0	10
30	Scaled conductance quantization unravels the switching mechanism in organic ternary resistive memories. Journal of Materials Chemistry C, 2020, 8, 2964-2969.	5.5	5
31	Structure of the RNA-dependent RNA polymerase from COVID-19 virus. Science, 2020, 368, 779-782.	12.6	1,228
32	Biodiversity Survey of Flower-Visiting Spiders Based on Literature Review and Field Study. Environmental Entomology, 2020, 49, 673-682.	1.4	7
33	Structures of cell wall arabinosyltransferases with the anti-tuberculosis drug ethambutol. Science, 2020, 368, 1211-1219.	12.6	82
34	Structure-based design of antiviral drug candidates targeting the SARS-CoV-2 main protease. Science, 2020, 368, 1331-1335.	12.6	1,135
35	Advances in Toxicological Research of the Anticancer Drug Cisplatin. Chemical Research in Toxicology, 2019, 32, 1469-1486.	3.3	215
36	Organometallic ruthenium anticancer complexes inhibit human peroxiredoxin I activity by binding to and inducing oxidation of its catalytic cysteine residue. Metallomics, 2019, 11, 546-555.	2.4	8

ΥΑΟ ΖΗΑΟ

#	Article	IF	CITATIONS
37	Crystal Structures of Membrane Transporter MmpL3, an Anti-TB Drug Target. Cell, 2019, 176, 636-648.e13.	28.9	172
38	A negatively charged Pt(<scp>iv</scp>) prodrug for electrostatic complexation with polymers to overcome cisplatin resistance. Journal of Materials Chemistry B, 2019, 7, 3346-3350.	5.8	27
39	Proteomic Strategy for Identification of Proteins Responding to Cisplatin-Damaged DNA. Analytical Chemistry, 2019, 91, 6035-6042.	6.5	14
40	In Situ Liquid Secondary Ion Mass Spectrometry: A Surprisingly Soft Ionization Process for Investigation of Halide Ion Hydration. Analytical Chemistry, 2019, 91, 7039-7046.	6.5	27
41	Mass spectrometric quantification of the binding ratio of metalâ€based anticancer complexes with protein thiols. Rapid Communications in Mass Spectrometry, 2019, 33, 951-958.	1.5	3
42	Uptake and Transformation of Silver Nanoparticles and Ions by Rice Plants Revealed by Dual Stable Isotope Tracing. Environmental Science & Technology, 2019, 53, 625-633.	10.0	52
43	Potential-Dynamic Surface Chemistry Controls the Electrocatalytic Processes of Ethanol Oxidation on Gold Surfaces. ACS Energy Letters, 2019, 4, 215-221.	17.4	45
44	A Photoactive Platinum(IV) Anticancer Complex Inhibits Thioredoxin–Thioredoxin Reductase System Activity by Induced Oxidization of the Protein. Inorganic Chemistry, 2018, 57, 5575-5584.	4.0	24
45	Snapshots of catalysis: Structure of covalently bound substrate trapped in Mycobacterium tuberculosis thiazole synthase (ThiG). Biochemical and Biophysical Research Communications, 2018, 497, 214-219.	2.1	2
46	Solvent-dependent structural dynamics of an azido-platinum complex revealed by linear and nonlinear infrared spectroscopy. Physical Chemistry Chemical Physics, 2018, 20, 9984-9996.	2.8	8
47	Heterogeneous Reaction of HCOOH on NaCl Particles at Different Relative Humidities. Journal of Physical Chemistry A, 2018, 122, 7218-7226.	2.5	3
48	Tea saponin reduces the damage of <i> Ectropis obliqua</i> to tea crops, and exerts reduced effects on the spiders <i>Ebrechtella tricuspidata</i> and <i> Evarcha albaria</i> compared to chemical insecticides. PeerJ, 2018, 6, e4534.	2.0	15
49	The gut microbiota in larvae of the housefly Musca domestica and their horizontal transfer through feeding. AMB Express, 2017, 7, 147.	3.0	49
50	Bt proteins Cry1Ah and Cry2Ab do not affect cotton aphid Aphis gossypii and ladybeetle Propylea japonica. Scientific Reports, 2016, 6, 20368.	3.3	24
51	Bacterial communities of the cotton aphid Aphis gossypii associated with Bt cotton in northern China. Scientific Reports, 2016, 6, 22958.	3.3	46
52	Impact of Single and Stacked Insect-Resistant Bt-Cotton on the Honey Bee and Silkworm. PLoS ONE, 2013, 8, e72988.	2.5	24
53	Hydrogen Isotope Effects on Aqueous Electrolyte for Electrochemical Lithiumâ€ion Storage. Angewandte Chemie, 0, , .	2.0	3